Communication

Functional Group Effects on the HOMO–LUMO Gap of g-C$_3$N$_4$

Hao Li [1,*,†], Zhien Zhang [2,*], Yulu Liu [3], Wanglai Cen [4] and Xubiao Luo [2]

1   College of Chemistry, Sichuan University, Chengdu 610064, China
2   Key Laboratory of Jiangxi Province for Persistant Pollutants Control and Resources Recycle,
    Nanchang Hangkong University, Nanchang 330063, China; luoxubiao@126.com
3   College of Architecture and Environment, Sichuan University, Chengdu 610064, China; yulu5412@126.com
4   Institute of New Energy and Low Carbon Technology, Sichuan University, Chengdu 610207, China;
    cenwl@utexas.edu
*   Correspondence: lihao@utexas.edu (H.L.); zhienzhang@cqut.edu.cn (Z.Z.)
†   Current Address: Department of Chemistry and Institute for Computational and Engineering Sciences,
    The University of Texas at Austin, 105 E. 24th Street, Stop A5300, Austin, TX 78712, USA.

check for updates

Abstract: Graphitic carbon nitride (g-C$_3$N$_4$) is a promising semiconductor material which has been widely studied in nanoscience. However, the effect of modifying the performance of g-C$_3$N$_4$ is still under debate. In this communication, we show the size and functional group effects on the g-C$_3$N$_4$ using density functional theory (DFT) calculations. It was found that a molecule with six repeated g-C$_3$N$_4$ units (g-C$_3$N$_4$-6) could be the smallest unit that converges to the limit of its HOMO–LUMO gap. Calculations of g-C$_3$N$_4$-6 with varying numbers of substituted C$\equiv$N, C=O, and O$-$H functional groups show that C$\equiv$N and C=O could narrow down the HOMO–LUMO gap, while O$-$H could slightly raise the gap. This study shows that the change of substituents could tune the band gap of g-C$_3$N$_4$, suggesting that rationally modifying the substituent at the edge of g-C$_3$N$_4$-based materials could help to significantly increase the photocatalytic properties of a metal-free g-C$_3$N$_4$.

1. Introduction

Graphitic carbon nitride (g-C$_3$N$_4$) is a promising metal-free polymeric n-type semiconductor which has attracted huge interest during the past decade [1–4]. With its important electric, optical, structural, thermal, and chemical properties, g-C$_3$N$_4$ has been widely applied to electro- and photo-chemistries. Since the primary works done by Wang et al. [5], which showed that g-C$_3$N$_4$ is a promising photocatalyst for hydrogen evolution under visible light, g-C$_3$N$_4$ has been widely studied as a cost-effective photocatalyst for many reactions, such as carbon dioxide reduction [6–8] and photodegradation [1,9–11]. From experimental measurements, the band gap of g-C$_3$N$_4$ is usually between 2–3 eV, which could enable it to harvest sunlight with a wavelength of around 460 nm [1,6]. However, this still deviates from the well-known ideal band gap of a semiconductor (around 2.0 eV). Therefore, slightly narrowing down the band gap of g-C$_3$N$_4$ would be a particularly challenging but important target in the material's modification.

To narrow down the band gap of g-C$_3$N$_4$-based materials, doping with transition metal ions has been proven as an efficient strategy (e.g., cave [12–14] and interlayer [15] dopings). However, such a method involves a transition metal as the experimental input, which could raise the cost for industrial applications. Therefore, metal-free band gap engineering is particularly important. Currently, it is not well-known as to whether some of the modified g-C$_3$N$_4$-like materials could perform enhanced photocatalytic activities

compared to pure g-C$_3$N$_4$. A better understanding of the mechanisms of band gap tuning would be beneficial to the future design and understanding of high-performance modified g-C$_3$N$_4$ materials.

In this paper, we examine how the HOMO−LUMO gap changes with the g-C$_3$N$_4$ size and correlates with the substituted functional group using density functional theory (DFT) calculations. The functional group effect on g-C$_3$N$_4$ with different substituted functional groups was studied, and the HOMO−LUMO gaps of g-C$_3$N$_4$ with varying numbers of C≡N, C=O, and O−H groups were calculated. For the first time, we found that g-C$_3$N$_4$ with a specific amount of substituted C≡N or C=O could narrow down the HOMO−LUMO gap; a finding which could impart significant guidance to g-C$_3$N$_4$ band gap engineering.

2. Computational Method

All the DFT calculations were performed to calculate the HOMO−LUMO gap with the Vienna Ab initio simulation package (VASP) [16]. Electron-core interactions were described within the projector-augmented wave (PAW) method [17]. Generalized-gradient approximation (GGA) with the Perdew–Burke–Ernzerhof (PBE) functional was performed for electron exchange and correlation [18]. Kohn–Sham orbitals were expanded on a plane-wave basis [19]. The kinetic energy cutoff was set as 400 eV for all the calculations. All the configurations were considered optimal when all the forces on each atom were lower than 0.05 eV/Å. The Brillouin zone was sampled by Γ-point. The vacuum of at least 10 Å was set in the z-dimension. The lengths of the x- and y-dimensions ranged from 20 to 40 Å for the g-C$_3$N$_4$ structures with varying size. Convergence tests with higher kinetic energy cutoff and lower forces were performed; no significant change was found in the results.

3. Results and Discussion

Here, we performed DFT calculations to elucidate the effects of size and functional groups on the HOMO−LUMO gap of g-C$_3$N$_4$ structures. We first studied the size effect on the pure g-C$_3$N$_4$. Figure 1 shows that the HOMO−LUMO gap monotonically decreases with the increase of g-C$_3$N$_4$ repeated units and then reaches a plateau, suggesting that if the size is sufficiently large, the HOMO–LUMO gap becomes less sensitive to size. This is quite similar to a previous theoretical study on nanographene structures by Jiang and Dai [20]: there should be a critical size that leads to a convergence of the HOMO−LUMO gap of graphene or graphene-like materials.
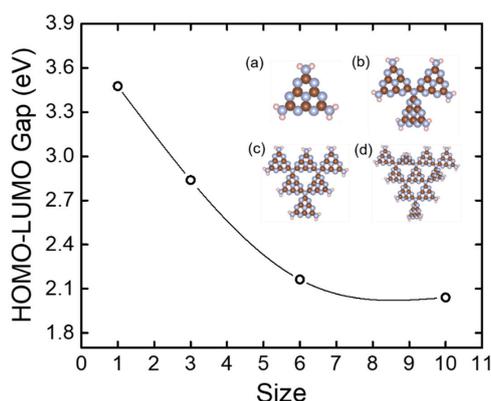
Figure 1. Calculated HOMO–LUMO gap vs g-C$_3$N$_4$ structures with varying sizes. Insets show the optimized configurations of (**a**) g-C$_3$N$_4$-1; (**b**) g-C$_3$N$_4$-3; (**c**) g-C$_3$N$_4$-6; and (**d**) g-C$_3$N$_4$-10. Brown, blue, and pink spheres represent C, N, and H, respectively.

With the conclusion from Figure 1, that a g-C$_3$N$_4$ structure with six repeated g-C$_3$N$_4$ units (g-C$_3$N$_4$-6) is large enough to represent a periodic structure, all further calculations were performed with this critical size. Figure 2 shows the tuning of the HOMO−LUMO gap with the increasing number of C≡N, C=O, and O−H in a g-C$_3$N$_4$-6 structure (the structural information can be found in

Figures 3–5). Interestingly, although all of the three trends are not monotonic, they generally show that the existence of C≡N and C=O can significantly narrow down the HOMO–LUMO gap, while O−H can slightly raise the gap. The differences on the effects of functional groups might originate from the different electronic properties among the functional groups: O−H is electron-donating, while C≡N and C=O are electron-withdrawing. Tian et al. [21] suggested that substitutes with electron-donating and -withdrawing properties could lead to the different distribution of HOMO and LUMO. In this study, our results suggest that the form of carbon and oxygen contained in the g-C_3N_4 are particularly important: for a g-C_3N_4 structure, a certain ratio of C≡N and C=O may narrow down the energy band gap to the optimized value, leading to higher photocatalytic performance. From an experimental perspective, it is expected that the preparation of g-C_3N_4 substituted with more electron-withdrawing groups could be beneficial to both scientific and industrial applications.
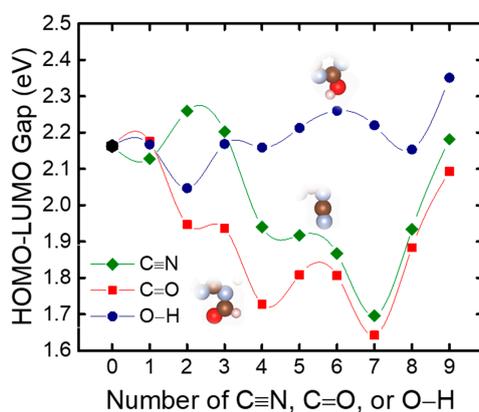
Figure 2. Calculated HOMO–LUMO gap vs a g-C_3N_4-6 structure with varying numbers of C≡N, C=O, and O−H. Configurations used for DFT calculations are shown in Figures 3–5. Insets show the functional groups in the calculated configurations. Brown, blue, pink, and red spheres represent C, N, H, and O, respectively.
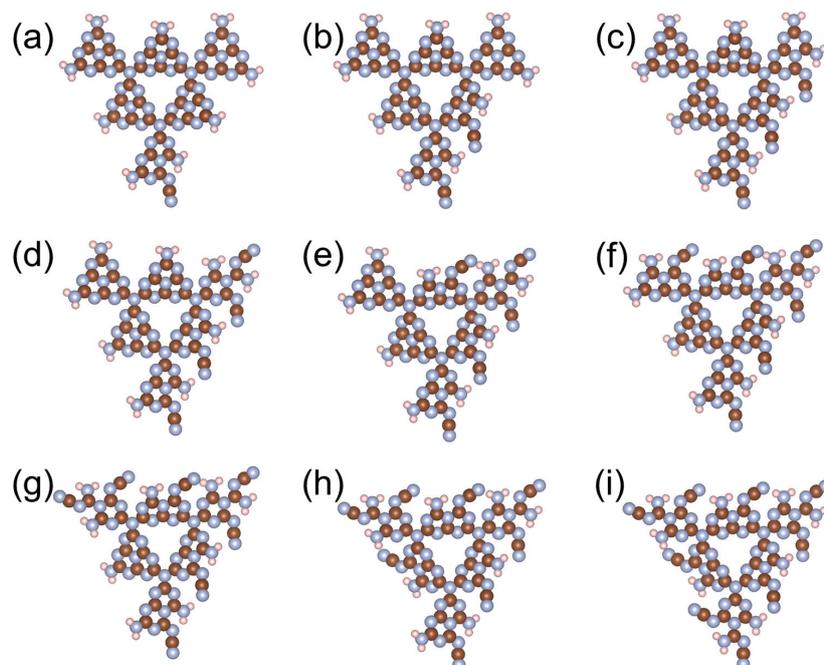
Figure 3. Structures of g-C_3N_4-6 with varying numbers of C≡N groups. Brown, blue, and pink spheres represent C, N, and H, respectively.
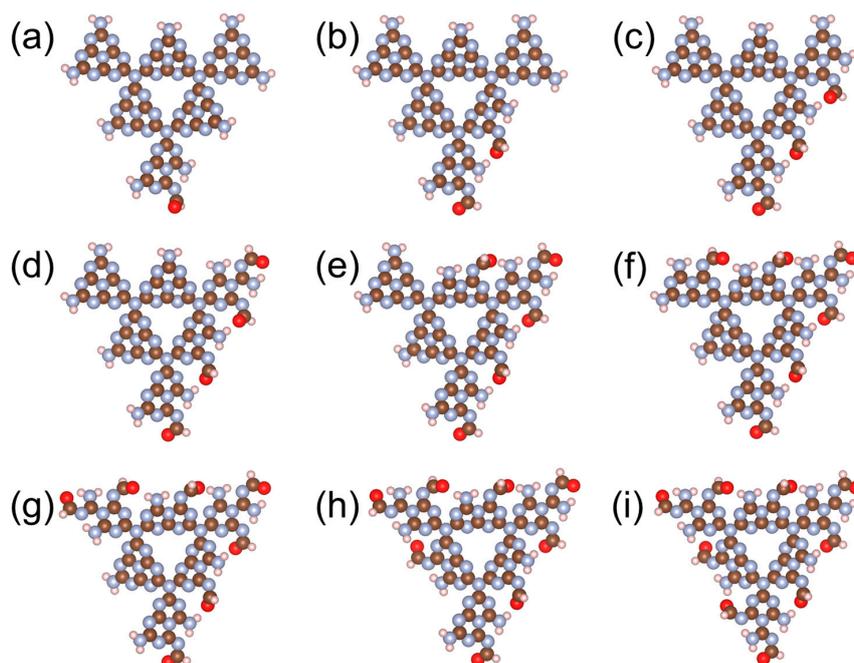
Figure 4. Structures of g-C_3N_4-6 with varying numbers of C=O groups. Brown, blue, pink, and red spheres represent C, N, H, and O, respectively.
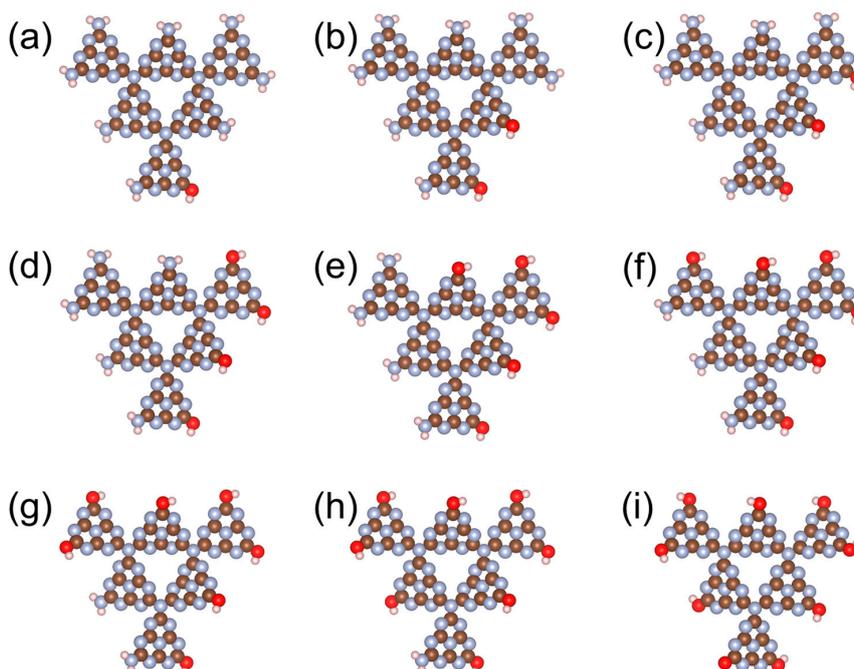
Figure 5. Structures of g-C_3N_4-6 with varying numbers of O−H groups. Brown, blue, pink, and red spheres represent C, N, H, and O, respectively.

4. Conclusions

In this communication, we have shown the size and functional group effects on g-C_3N_4 using DFT calculations. It was found that a g-C_3N_4-6 molecule could be the smallest unit that converges to the limit of the HOMO–LUMO gap. Calculations of g-C_3N_4-6 with varying numbers of substituted C≡N, C=O, and O−H functional groups have shown that generally, C≡N and C=O could narrow down the HOMO–LUMO gap, while O−H could slightly raise the gap. This study shows that rationally

modifying the substituent at the edge of g-C$_3$N$_4$-based materials during band gap engineering could help to increase the catalytic performance. In future studies, we will focus on revealing more physical understanding behind these functional group effects.

Conflicts of Interest: The authors declare no conflict of interest.

References

1. Wen, J.; Xie, J.; Chen, X.; Li, X. A review on g-C$_3$N$_4$-based photocatalysts. *Appl. Surf. Sci.* **2017**, *391*, 72–123. [CrossRef]
2. Cao, S.; Yu, J. G-C$_3$N$_4$-based photocatalysts for hydrogen generation. *J. Phys. Chem. Lett.* **2014**, *5*, 2101–2107. [CrossRef] [PubMed]
3. Groenewolt, M.; Antonietti, M. Synthesis of g-C$_3$N$_4$ nanoparticles in mesoporous silica host matrices. *Adv. Mater.* **2005**, *17*, 1789–1792. [CrossRef]
4. Fu, J.; Yu, J.; Jiang, C.; Cheng, B. g-C$_3$N$_4$-Based Heterostructured Photocatalysts. *Adv. Energy Mater.* **2018**, *8*. [CrossRef]
5. Wang, X.; Maeda, K.; Thomas, A.; Takanabe, K.; Xin, G.; Carlsson, J.M.; Domen, K.; Antonietti, M. A metal-free polymeric photocatalyst for hydrogen production from water under visible light. *Nat. Mater.* **2009**, *8*, 76–80. [CrossRef] [PubMed]
6. Ye, S.; Wang, R.; Wu, M.; Yuan, Y. A review on g-C$_3$N$_4$ for photocatalytic water splitting and CO$_2$ reduction. *Appl. Surf. Sci.* **2015**, *358*, 15–27. [CrossRef]
7. Shi, H.; Chen, G.; Zhang, C.; Zou, Z. Polymeric g-C$_3$N$_4$ coupled with NaNbO$_3$ nanowires toward enhanced photocatalytic reduction of CO$_2$ into renewable fuel. *ACS Catal.* **2014**, *4*, 3637–3643. [CrossRef]
8. Fu, J.; Zhu, B.; Jiang, C.; Cheng, B.; You, W.; Yu, J. Hierarchical Porous O-Doped g-C$_3$N$_4$ with Enhanced Photocatalytic CO$_2$ Reduction Activity. *Small* **2017**, *13*, 1–9. [CrossRef] [PubMed]
9. Yan, S.C.; Li, Z.S.; Zou, Z.G. Photodegradation performance of g-C$_3$N$_4$ fabricated by directly heating melamine. *Langmuir* **2009**, *25*, 10397–10401. [CrossRef] [PubMed]
10. Yan, S.C.; Li, Z.S.; Zou, Z.G. Photodegradation of Rhodamine B and Methyl Orange over Boron-Doped g-C$_3$N$_4$ under Visible Light Irradiation. *Langmuir* **2010**, *26*, 3894–3901. [CrossRef] [PubMed]
11. Ge, L.; Han, C.; Liu, J. Novel visible light-induced g-C$_3$N$_4$/Bi$_2$WO$_6$ composite photocatalysts for efficient degradation of methyl orange. *Appl. Catal. B Environ.* **2011**, *108–109*, 100–107. [CrossRef]
12. Cao, S.; Low, J.; Yu, J.; Jaroniec, M. Polymeric Photocatalysts Based on Graphitic Carbon Nitride. *Adv. Mater.* **2015**, *27*, 2150–2176. [CrossRef] [PubMed]
13. Chen, X.; Zhang, J.; Fu, X.; Antonietti, M.; Wang, X. Fe-g-C$_3$N$_4$-catalyzed oxidation of benzene to phenol using hydrogen peroxide and visible light. *J. Am. Chem. Soc.* **2009**, *131*, 11658–11659. [CrossRef] [PubMed]
14. Ge, L.; Han, C.; Liu, J.; Li, Y. Enhanced visible light photocatalytic activity of novel polymeric g-C$_3$N$_4$ loaded with Ag nanoparticles. *Appl. Catal. A Gen.* **2011**, *409–410*, 215–222. [CrossRef]
15. Xiong, T.; Cen, W.; Zhang, Y.; Dong, F. Bridging the g-C$_3$N$_4$ Interlayers for Enhanced Photocatalysis. *ACS Catal.* **2016**, *6*, 2462–2472. [CrossRef]
16. Hafner, J. Ab-initio simulations of materials using VASP: Density-functional theory and beyond. *J. Comput. Chem.* **2008**, *29*, 2044–2078. [CrossRef] [PubMed]
17. Blöchl, P.E. Projector augmented-wave method. *Phys. Rev. B* **1994**, *50*, 17953–17979. [CrossRef]
18. Perdew, J.P.; Burke, K.; Ernzerhof, M. Generalized Gradient Approximation Made Simple. *Phys. Rev. Lett.* **1996**, *77*, 3865–3868. [CrossRef] [PubMed]
19. Kohn, W.; Sham, L.J. Self-consistent equations including exchange and correlation effects. *Phys. Rev.* **1965**, *140*. [CrossRef]

20. Jiang, D.; Dai, S. Circumacenes versus periacenes: HOMO-LUMO gap and transition from nonmagnetic to magnetic ground state with size. *Chem. Phys. Lett.* **2008**, *466*, 72–75. [CrossRef]

21. Tian, H.; Yang, X.; Cong, J.; Chen, R.; Teng, C.; Liu, J.; Hao, Y.; Wang, L.; Sun, L. Effect of different electron donating groups on the performance of dye-sensitized solar cells. *Dyes Pigment.* **2010**, *84*, 62–68. [CrossRef]